XIX. MINERALOGY OF MANGANESE NODULES FROM THE GH79-1 AREA

Kokichi Iizasa

Introduction

Petrographical and mineralogical investigations were made on manganese nodules from the GH79–1 area of the central Pacific by means of reflecting and transmitting microscopes, X-ray powder diffraction, electron microprobe analysis (EMX-SM), and microspectrophotometry (MMSP-PK).

Manganese and iron minerals of marine manganese nodules have not been well characterized due to their low crystallinity and small size of crystal. Terminology of the minerals is therefore controvercial as discussed by BURNS and BURNS (1977). BUSER and GRÜTTER (1956) first described 10Å manganite, 7Å manganite, and δ-MnO_2 as the constituent minerals of manganese nodules. Later those minerals were compared to the known minerals from land, todorokite (for 10Å manganite) and birnessite (for 7Å manganite and δ-MnO_2), on the basis of X-ray powder pattern (CRONAN and TOOMS, 1969; GLASBY, 1972). USUI *et al.* (1978) and USUI (1979) argued that major constituents of nodules are 10Å manganite and 2 line-form δ-MnO_2, and existence of 7Å manganite is very doubtful. In this article the terms 10Å manganite and 2 line-form δ-MnO_2 are used under the definition by BUSER and GRÜTTER (1956) and USUI (1979).

Ferromanganese minerals

Typical X-ray powder diffraction patterns of deep-sea manganese nodules from the survey area and synthetic 10Å manganite are illustrated in Fig. XIX-1.

10Å manganite occurs in nodules with rough surface (r-type nodules) more abundantly than those with smooth surface (s-type nodules), and does mainly in those semi-buried in siliceous clay and ooze. Nodules which occur in calcareous ooze and pelagic clay (occasionally zeolitic) almost consist of δ-MnO_2* (Sts. 1499, 1472, and 1452A).

Under a reflecting microscope, ferromanganese layers of the nodules from the survey area can be distinguished into the 10Å manganite and δ-MnO_2 zones (USUI *et al.*, 1978).

The 10Å manganite zone is an aggregate of hydrous manganese oxide mineral, 10Å manganite. It shows some characteristic textures such as cusps, veinlet, thin layer (Fig. XIX-2), massive form, and network, as described by USUI (1979). The veinlets cut the other textures and fill cracks.

Reflectivity of the 10Å manganite zone is not always consistent but show considerable fluctuation from 9.4 to 13.5 per cent (560 nm in air). The results of electron microprobe analysis (EPMA) suggest that this fluctuation is caused by the varying content of amorphous iron hydroxide (Table XIX-1). Iron content of high-reflectivity zone (reflectivity: 12.9 to 13.5 per cent) is around 2%, whereas that of low-reflectivity zone (reflectivity:

*2 line-form δ-MnO_2 is abbreviated as δ-MnO_2 for convenience in the following description.

9.4 to 11.8 per cent) is more than 5%. The two zones are transitional to each other or discretely distributed in nodules. Manganese, copper, nickel, and magnesium are more concentrated in the 10Å manganite zone than in the δ-MnO_2 zone (Table XIX-1). The

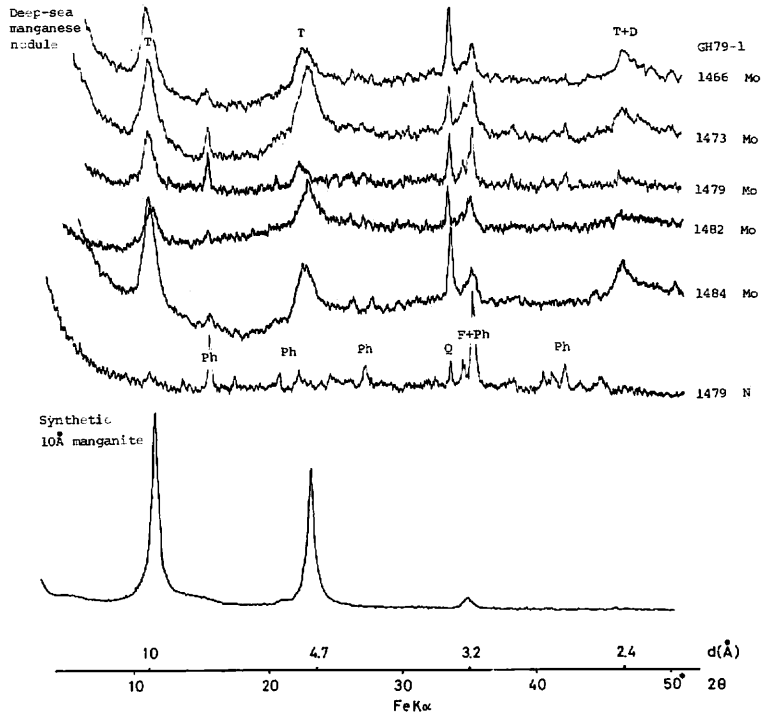

Fig. XIX-1 X-ray powder diffraction patterns of the manganese nodules from the Central Pacific Basin and synthetic 10Å manganite. T; 10Å manganite, D; δ-MnO_2, Q; quartz, F; plagioclase, Ph; phillipsite, Mo; manganese oxide zone, Wn; whole nodule, N; nucleus of nodule.

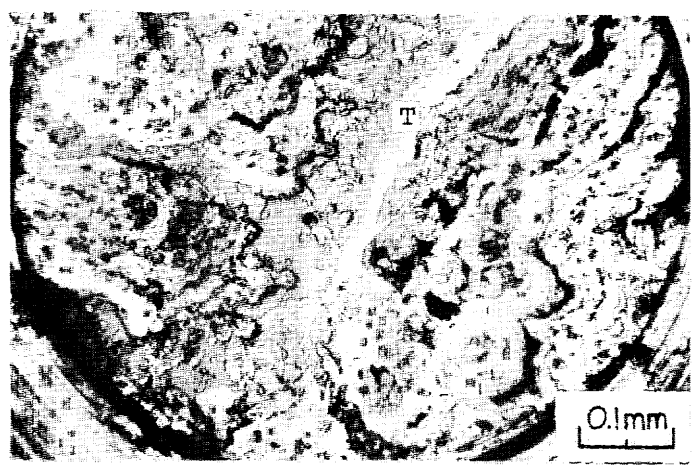

Fig. XIX-2 10Å manganite zone of fissure filling veinlet and thin film type in reflected light (St. 1473). T; 10Å manganite zone.

Table XIX-1 Chemical composition of high reflectivity 10Å manganite zone (A), low reflectivity 10Å manganite zone (B) and δ-MnO_2 zone in nodules by electron microprobe analyses.

	Mn	Fe	Co	Ni	Cu
A	35.84 ±4.91	1.81 ±1.13	0.27 ±0.15	2.30 ±0.55	1.44 ±0.43
B	24.07 ±2.08	7.77 ±1.80	0.61 ±0.21	1.94 ±0.51	1.01 ±0.22
δ-MnO_2 zone	25.19 ±3.57	10.38 ±1.29	0.37 ±0.09	0.85 ±0.61	0.25 ±0.15

	Ca	Mg	Al	Si	K	Ti
A	0.97 ±0.26	4.23 ±0.93	2.92 ±1.46	1.69 ±1.08	0.39 ±0.18	0.24 ±0.22
B	1.18 ±0.28	3.10 ±1.01	2.87 ±0.62	3.58 ±0.95	0.33 ±0.10	0.19 ±0.19
δ-MnO_2 zone	1.65 ±0.20	1.49 ±0.50	1.09 ±0.47	2.66 ±0.64	0.35 ±0.06	0.81 ±0.09

(Average and standard deviation in weight %)

10Å manganite zone may be a submicroscopic mixture of 10Å manganite and minor amount of amorphous iron hydroxide.

The δ-MnO_2 zone is characterized by columnar texture (Fig. XIX-3) which includes various kinds of silicate minerals (quartz, plagioclase, olivine-like minerals, etc.), amorphous Fe–Mn hydroxides and microfossils (indeterminable). The zone is dark grey. Its reflectivity is lower than that of the 10Å manganite zone and is approximately 7.9% (560 nm in air). Iron content of the zone is about 10% (Table XIX-1).

Accessory minerals

Accessory minerals are quartz, plagioclase, phillipsite, chalcedony, apatite, olivine-like mineral, and hematite Table XIX-2).

Quartz with angular form and chalcedony (Figs. XIX-4, 6) are abundant in both the ferromanganese layers and nuclei of nodules. Plagioclase is generally in euhedral form (Fig. XIX-5). Radial aggregations of euhedral crystals of phillipsite are observed in the ferromanganese layers and cracks of almost all nodules (Fig. XIX-7).

Altered olivine-like minerals (Fig. XIX-8) occur in the ferromanganese layers and nuclei of the nodules near seamounts (Table XIX-2). Hematite is observed in the nuclei of the nodules also near a seamount (St. 1479).

Besides the minerals above described, there are many small projections of unknown minerals perpendicular to the wall of cracks (Fig. XIX-9).

Acknowledgments

The author is grateful to Dr. A. Usui for his critical reading of the manuscript.

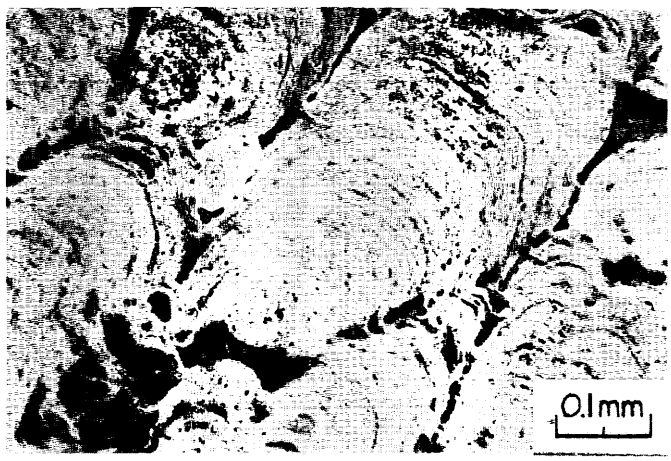

Fig. XIX-3 δ-MnO_2 zone of columnar strycture in reflected light (St. 1479).

References

BUSER, W. and CRÜTTER, A. (1956) Über die Natur der Manganknollen. *Schwiz. Mineral. Petrogr. Mitt.*, vol. 36, p. 49–62.

CRONAN, D. S. and TOOMS, J. S. (1969) The geochemistry of manganese nodules and associated pelagic deposits from the Pacific and Indian Oceans. *Deep-Sea Res.*, vol. 16, p. 335–359.

GLASBY, G. P. (1972) The mineralogy of manganese nodules from a range of marine environments. *Mar. Geol.*, vol. 13, p. 57–72.

USUI, A. (1979) Minerals, metal contents, and mechanism of formation of manganese nodules from the Central Pacific Basin (GH76–1 and GH77–1 areas). *In* BISCHOFF, J. L. and PIPER, D. Z. (*eds.*), *Marine Geology and Oceanography of the Pacific Manganese Nodule Province*, Plenum Publishing Co., p. 651–679.

————, TAKENOUCHI, S., and SHOJI, T. (1978) Mineralogy of deep sea manganese nodules and synthesis of manganese oxides: implications to genesis and geochemistry. *Mining Geology*, vol. 28, p. 405–420.

Table XIX-2 Mineral constituents of deep-sea manganese nodules of the GH79-1 cruise by X-ray powder diffraction analyses and microscopic observations.

St. No.	Sp. No.	T	D	Q	Pl	Ph	Ol	Others
1448	GB915	+	±	+	+	+	N.D.	
1449	GB916A	−	++	+	+	+	−	
1452	GB919	+	++	+	+	+	N.D.	
1453	GB920	+	++	+	+	+	+	
1454	GB921	+	++	+	+	+	N.D.	
1455	GB922	+	++	+	+	+	N.D.	
1456	FG123C1	+	+	+	+	+	N.D.	
1457	GB924	+	++	+	+	+	−	
1458	GB925	+	+	+	+	+	N.D.	
1459	GB926	+	++	+	+	+	N.D.	
1460	GB927	+	+	+	+	+	−	
1462	GB929	+	++	+	+	+	+	
1463	GB930	+	++	+	+	+	N.D.	
1464	GB931	+	++	+	+	+	±	
1465	GB932	+	++	+	+	+	N.D.	
1466	GB933	++	+	+	+	+	N.D.	
1469	FG136C1	++	+	+	+	+	N.D.	
1470	GB937	+	++	+	+	+	N.D.	
1471	FG138-1	+	+	+	+	+	N.D.	
1472	GB939	−	+	++	−	−	N.D.	
1473	GB940	++	+	+	+	+	N.D.	
1475	GB942	++	+	+	+	+	N.D.	
1476	GB'943	++	+	+	+	+	N.D.	
1477	GB944	++	+	+	+	+	−	
1479	GB946	++	+	+	+	+	−	hematite
1481	GB'948	++	++	+	+	+	N.D.	
1482	GB949	++	+	+	+	+	−	
1483	GB950	++	+	+	+	+	+	
1484	GB'951	++	+	+	+	+	−	
1481A1	FG154C1	+	++	+	+	+	−	
	C2	+	++	+	+	+	+	
	C3	+	++	+	+	+	++	
	C6	+	+	+	+	+	−	
	C7	++	+	+	+	+	−	
	C8	++	+	+	+	+	−	
	C9	++	+	+	+	+	−	
	C10	++	+	+	+	+	−	
1484A1	FG155C1	++	+	+	+	+	N.D.	
	C2	++	±	+	+	+	N.D.	
	C3	++	+	+	+	+	−	
1481A2	FG156C4	++	+	+	−	+	N.D.	
1452A	FG158C2	−	+	+	−	+	N.D.	
1487	FG159C1	+	+	+	+	+	N.D.	
1488	FG160C2	+	+	+	+	+	N.D.	
1489	GB953	+	+	+	+	+	N.D.	
1490	GB954	+	+	+	+	+	N.D.	
1491	GB955	+	+	+	+	+	N.D.	
1492	GB956	+	++	+	+	+	−	apatite

St. No.: station number Sp. No.: sample number T: 10Å manganite D: δ-MnO_2 Q: quartz Pl: plagioclase Ph: phillipsite Ol: olivine-like mineral N.D.: not determined ++: predominant +: dominant −: trace.

Fig. XIX-4a Parallel nicols. Q; Quartz.

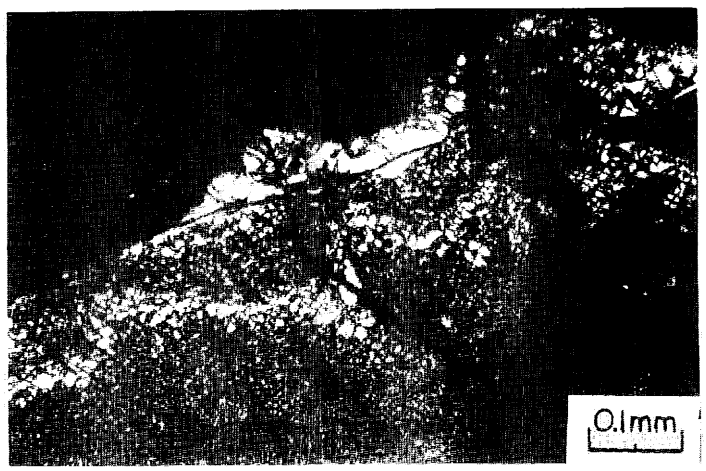

Fig. XIX-4b Crossed nicols. Photomicrographs showing cryptocrystalline quartz in nucleus of a deep-sea manganese nodule (St. 1477).

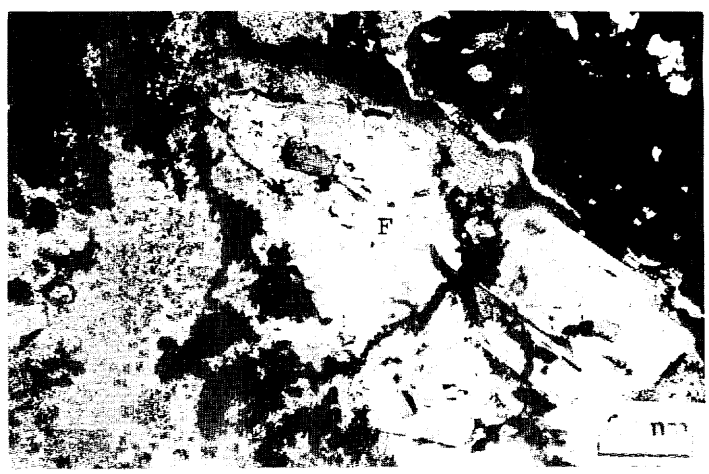

Fig. XIX-5a Parallel nicols. F; Plagioclase.

Fig. XIX-5b Crossed nicols. Photomicrographs showing large crystals of plagioclase in nodule (St. 1484 A-1).

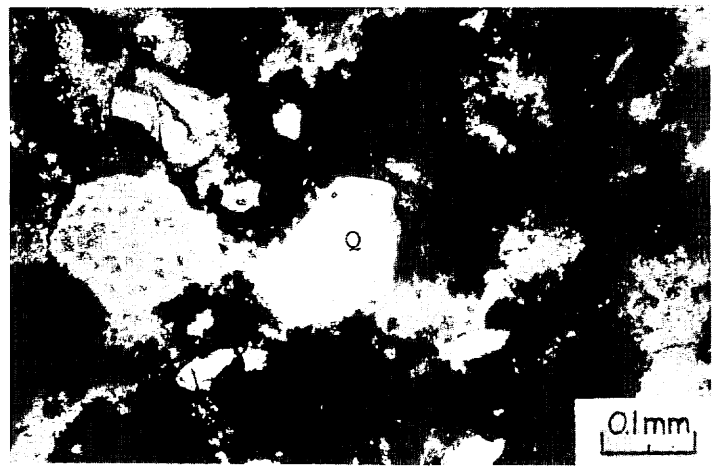

Fig. XIX-6 Quartz grain in the manganese oxide zone of the nodule (St. 1462) at parallel nicols.

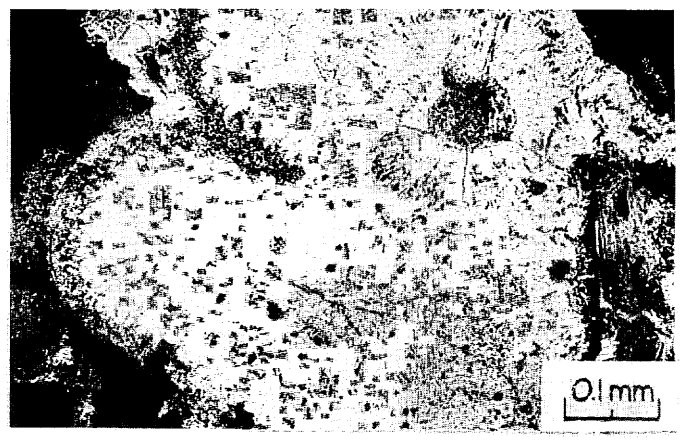

Fig. XIX-7 Zeolite forming nucleus of the nodule (St. 1479) at parallel nicols.

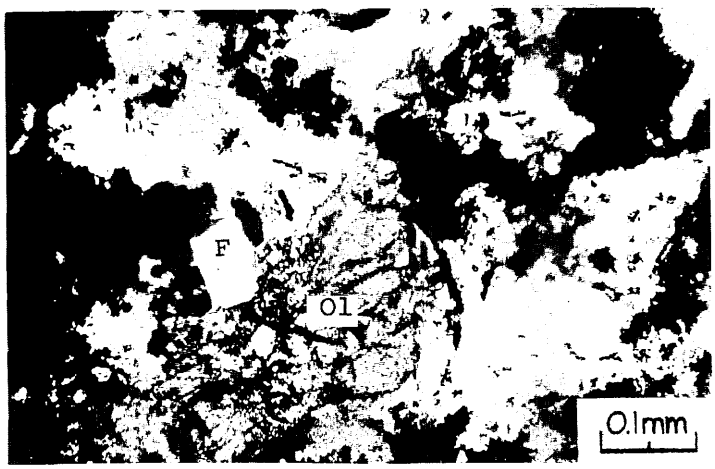

Fig. XIX-8a Parallel nicols. Ol; Olivine-like mineral.

Fig. XIX-8b Crossed nicols. Photomicrographs showing plagioclase and olivine-like mineral in the nodule (St. 1462).

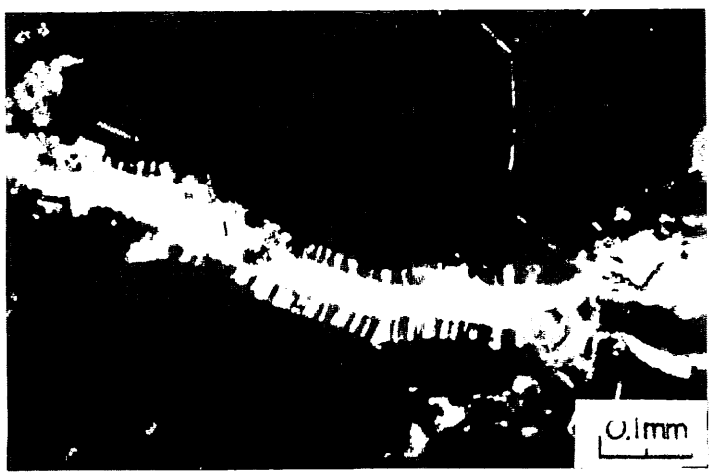

Fig. XIX-9 There are many tiny objects perpendicular to wall of fissure (St. 1492) at parallel nicols.